



ALMA MATER STUDIORUM
UNIVERSITÀ DI BOLOGNA

ARCHIVIO ISTITUZIONALE
DELLA RICERCA

Alma Mater Studiorum Università di Bologna Archivio istituzionale della ricerca

Polymers with Side Chain Porosity for Ultraparpermeable and Plasticization Resistant Materials for Gas Separations

This is the final peer-reviewed author's accepted manuscript (postprint) of the following publication:

Published Version:

Polymers with Side Chain Porosity for Ultraparpermeable and Plasticization Resistant Materials for Gas Separations / Yuan He, Francesco M. Benedetti, Sharon Lin, Chao Liu, Yanchuan Zhao, Hong-Zhou Ye, Troy Van Voorhis, Maria Grazia De Angelis, Timothy M. Swager, Zachary P. Smith. - In: ADVANCED MATERIALS. - ISSN 0935-9648. - STAMPA. - 31:21(2019), pp. 1807871.1-1807871.8. [10.1002/adma.201807871]

Availability:

This version is available at: <https://hdl.handle.net/11585/688299> since: 2019-05-31

Published:

DOI: <http://doi.org/10.1002/adma.201807871>

Terms of use:

Some rights reserved. The terms and conditions for the reuse of this version of the manuscript are specified in the publishing policy. For all terms of use and more information see the publisher's website.

This item was downloaded from IRIS Università di Bologna (<https://cris.unibo.it/>).
When citing, please refer to the published version.

(Article begins on next page)

DOI: 10.1002/((please add manuscript number))

Article type: Communication

Polymers with Side Chain Porosity for Ultrapерmeable and Plasticization Resistant Materials for Gas Separations

*Yuan He, Francesco M. Benedetti, Sharon Lin, Chao Liu, Yanchuan Zhao, Hong-Zhou Ye, Troy Van Voorhis, M. Grazia De Angelis, Timothy M. Swager and Zachary P. Smith**

Yuan He, Hong-Zhou Ye, Prof. Troy Van Voorhis, Prof. Timothy M. Swager

Department of Chemistry, Massachusetts Institute of Technology, Cambridge, Massachusetts 02139, USA

Francesco M. Benedetti, Sharon Lin, Prof. Zachary P. Smith*

Department of Chemical Engineering, Massachusetts Institute of Technology, Cambridge, Massachusetts 02139, USA

E-mail: zpsmith@mit.edu

Francesco M. Benedetti, Prof. M. Grazia De Angelis

Department of Civil, Chemical, Environmental, and Materials Engineering, University of Bologna, 40131 Bologna, Italy

Dr. Chao Liu, Prof. Yanchuan Zhao

This is the author manuscript accepted for publication and has undergone full peer review but has not been through the copyediting, typesetting, pagination and proofreading process, which may lead to differences between this version and the [Version of Record](#). Please cite this article as [doi: 10.1002/adma.201807871](https://doi.org/10.1002/adma.201807871).

This article is protected by copyright. All rights reserved.

Key Laboratory for Organofluorine Chemistry, Center for Excellence in Molecular Synthesis, Shanghai Institute of Organic Chemistry, University of Chinese Academy of Sciences, Chinese Academy of Sciences, 345 Ling-Ling Road, Shanghai 200032, China

Keywords: ROMP, gas separations, porous polymer, backbone flexibility, side chain rigidity

Abstract. Polymer membranes with ultrahigh CO₂ permeabilities and high selectivities are needed to address some of the critical separation challenges related to energy and the environment, especially in natural gas purification and post-combustion carbon capture. However, very few solution-processable, linear polymers are known today that access these types of characteristics, and all of the known structures achieve their separation performance through the design of rigid backbone chemistries that concomitantly increase chain stiffness and interchain spacing, thereby resulting in ultramicroporosity in solid-state chain-entangled films. Herein we report the separation performance of a porous polymer obtained via Ring-Opening Metathesis Polymerization (ROMP), which possesses a flexible backbone with rigid, fluorinated side chains. This polymer exhibits ultrahigh CO₂ permeability (> 21000 Barrer) and exceptional plasticization resistance (CO₂ plasticization pressure > 51 bar). Compared to traditional polymers of intrinsic microporosity (PIMs), the rate of physical aging is slower, especially for gases with small effective diameters (*i.e.*, He, H₂, and O₂). This structural design strategy, coupled with studies on fluorination, demonstrates a generalizable approach to create new polymers with flexible backbones and pore-forming side chains that have unexplored promise for small molecule separations.

Membranes are a promising platform technology for energy-efficient chemical separations. Unlike other separation processes, membranes do not require thermal regeneration, phase changes, or moving parts.^[1] Increasing the permeability of polymer membranes used for gas separations is essential for enhancing productivity and reducing membrane areas required for large-scale gas and vapor separations.^[2] Specific membrane applications include natural gas purification, hydrogen separations, air separation, and CO₂ capture from flue gas.^[3,4]

Over the past decade, polymers of intrinsic microporosity (PIMs) have defined the state-of-the-art for gas separations.^[5,6] Their rigid and contorted backbone structures lead to excellent separation performance for a variety of challenging binary separations (*e.g.*, CO₂/N₂, CO₂/CH₄, O₂/N₂,

This article is protected by copyright. All rights reserved.

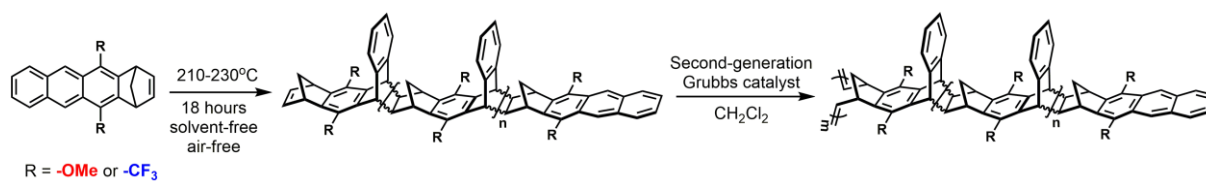
and H₂/CH₄).^[5] Guided by the discovery that polymers of intrinsic microporosity^[7] now called PIMs were highly effective for gas separation,^[8] researchers have sought to extend the database of accessible structures by designing and synthesizing ladder-type porous polymers containing more rigid backbones with even less conformational freedom.^[9,10] Despite the advances in backbone rigidity of polymer chains, a relatively unexplored design strategy of creating porous polymers is to attach rigid, free-volume-generating sidechains to a flexible backbone to form a type of “bottlebrush” polymer. Recently, some of us have found that these polymers can be highly porous as a result of inefficient packing between rigid, non-compliant side chains.^[11] In addition, since rigid macromonomers containing polymerizable units are synthesized before polymerization (**Scheme 1a**), it is easier to incorporate a variety of unique and pre-designed functionalities into this class of polymer as compared to PIM-1, which mainly relies on post-polymerization functionalization.^[12,13] From a transport perspective, pre-designing side-chain structures can enhance the entropic ordering of ultramicropores, enabling easier access to controlled entropic selectivities that are not currently considered from the activated state theory approach used to define the current polymer upper bound.^[14]

It is well-known that fluorinated polymers introduce properties such as thermal stability and non-wettability, which have enabled commercial applications.^[15] In terms of gas separation, previous studies have shown that the introduction of fluorinated moieties in aromatic polyimides can dramatically increase gas permeability with little impact on permselectivity.^[16] In poly(organosiloxanes), it was found that CO₂ permeability and CO₂/CH₄ selectivity could increase simultaneously by incorporating fluorine-containing groups.^[17] In all these cases, bulky hexafluoroisopropylidene functionality is used to contort the polymer backbone and generate free

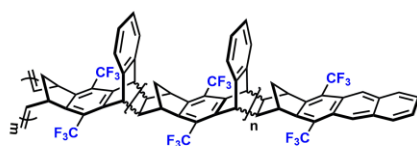
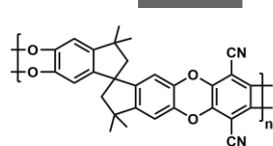
volume, thereby enhancing separation performance. Considering the synthetic versatility of using pore-forming macromonomers, the approach presented here enables a systematic comparison for studying the effect of fluorination on gas transport properties relative to that of hydrocarbon analogs in pre-designed ultramicropores. By doing so, a more direct deconvolution of the morphological and electronic contributions of fluorinated functionality on gas transport can be achieved.

This communication describes the gas transport properties of two porous polymers obtained via Ring-Opening Metathesis Polymerization (ROMP), which both possess flexible poly(norbornene) backbones with rigid side chains. Films of CF₃-ROMP exhibited ultrahigh CO₂ permeability (> 21000 Barrer) and exceptional plasticization resistance (CO₂ plasticization pressure > 51 bar). The structures of two porous ROMP polymers are shown in **Scheme 1b** and are based on synthetic procedures published previously.^[11] Side chains are made via an iterative Diels-Alder reaction, which generates a mixture of oligomers with different chain lengths (typically with 2-9 repeating units) (**Figure S1** and **S2**). The mixture of oligomers is directly used for ROMP polymerization. Schematic representations of CF₃-ROMP are shown in **Scheme 1c**. Both CF₃-ROMP and OMe-ROMP are readily soluble in common organic solvents, allowing characterization by NMR and GPC (**Figure S3** and **S4**). The pre-casting CF₃-ROMP and OMe-ROMP powder showed significant microporosity via N₂ adsorption isotherms at 77 K, with a Brunauer–Emmett–Teller (BET) surface area of 700 m² g⁻¹ and 146 m² g⁻¹, respectively (**Figure S6**). Solution casting from chloroform led to optically clear films (**Figure S9**) suitable for gas permeation studies.

a)



b)



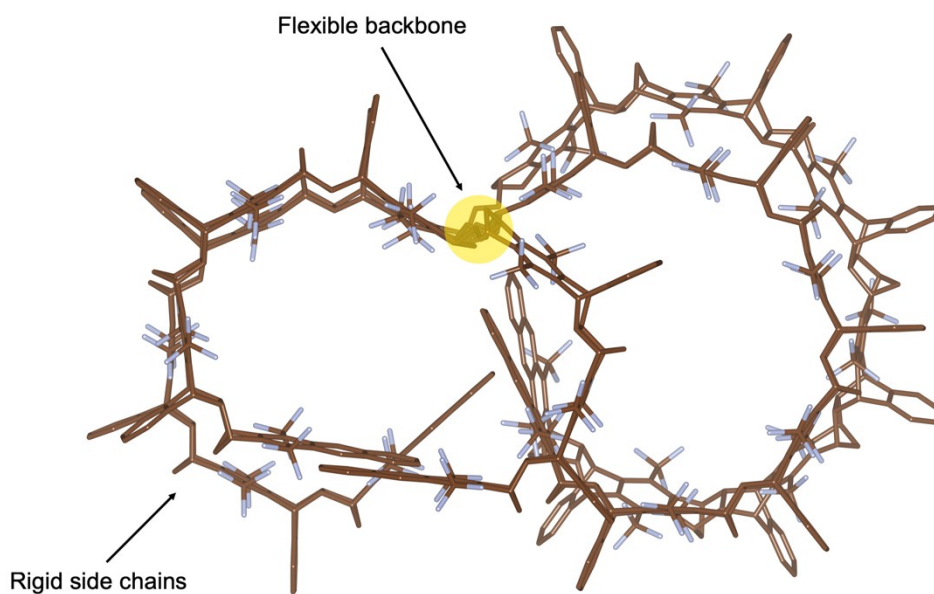
PIM-1

CF₃-ROMP

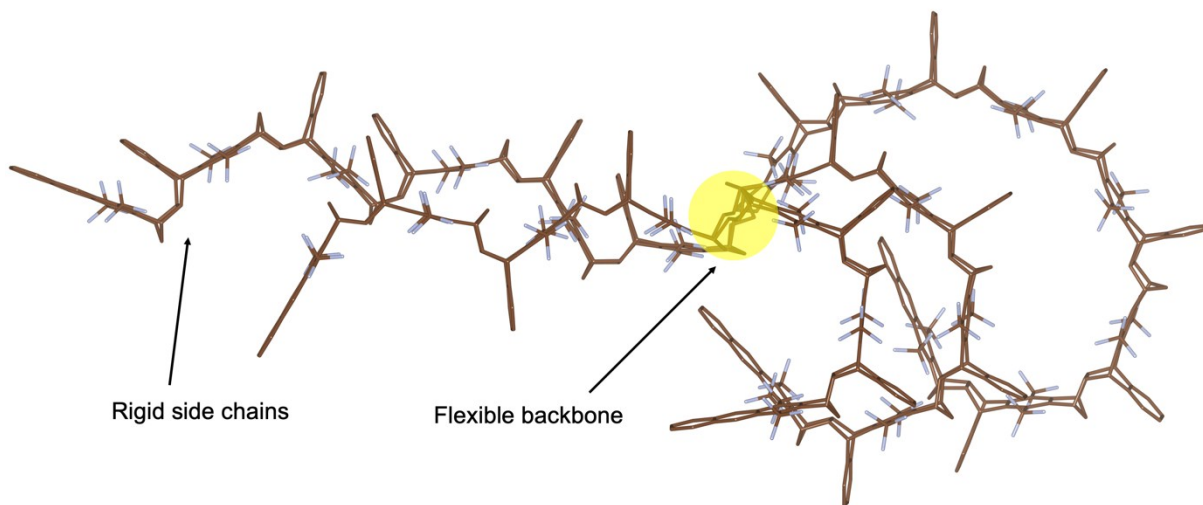
OMe-ROMP

Author Manuscript

c)

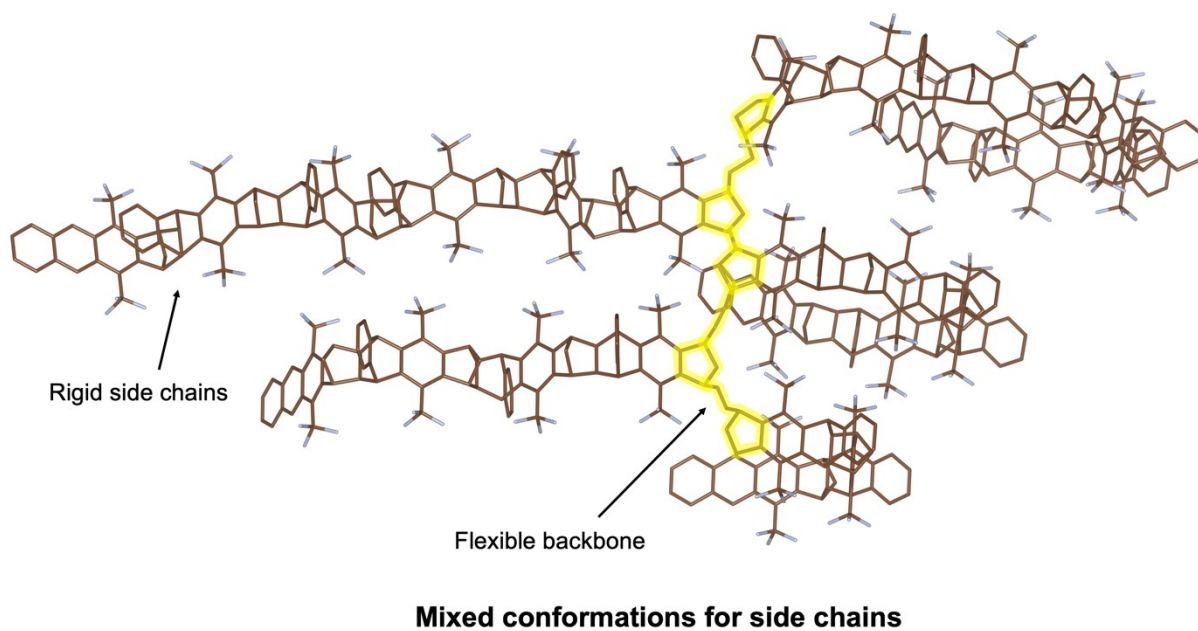
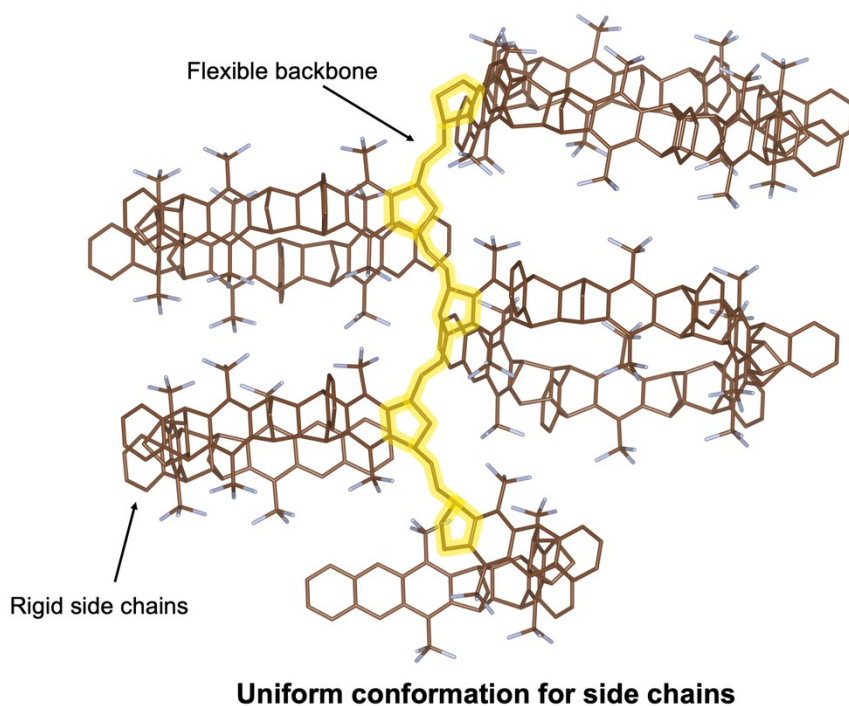


Uniform conformation for side chains



Mixed conformations for side chains

Auth



Scheme 1. a) Generalized synthetic procedure for CF_3 -ROMP and OMe-ROMP b) Molecular structures of PIM-1, CF_3 -ROMP, and OMe-ROMP c) Schematic representation of CF_3 -ROMP with 5 repeating units (uniform conformation or mixed conformations for side chains).

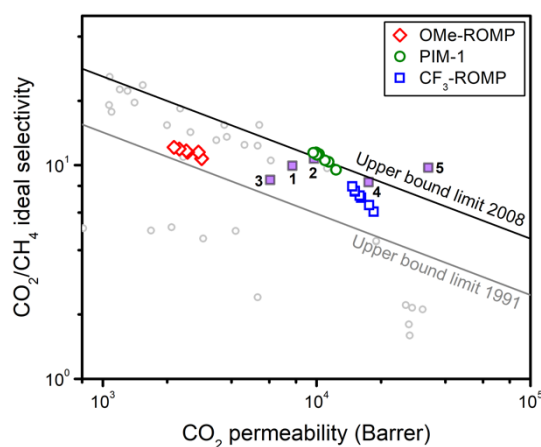
This article is protected by copyright. All rights reserved.

The gas separation performance of CF₃-ROMP, OMe-ROMP, and PIM-1 are shown in **Figure 1** and **Table S1**. Before permeation experiments, films were first soaked in ethanol for 48 h, dried at ambient conditions for 24 h, and then degassed in full vacuum for 8 h at 35 °C to remove residual solvent, as confirmed by TGA (**Figure S10**).^[18] The effect of different treatment conditions and film history were also investigated (Section 7, ESI). The magnitude of gas permeability for CF₃-ROMP and OMe-ROMP followed the order of CO₂ > H₂ > O₂ > He > CH₄ > N₂, indicating a strong solubility contribution to permeation (**Figure S11a**). CF₃-ROMP exhibited exceptionally high gas permeabilities across all gases tested, notably for CO₂ (~21300 Barrer) and H₂ (~8300 Barrer) for the non-aged film. These gas permeabilities were about 60 to 200% higher than the non-aged PIM-1 film under the same ethanol treatment and testing conditions, which makes CF₃-ROMP the third most permeable linear ultramicroporous polymer reported to date, behind PTMSP and PIM-TMN-Trip reported by Rose *et al.*^[9] As a result, CF₃-ROMP surpassed the 2008 Robeson upper bound for H₂/CH₄ after physical aging, and was above the 1991 Robeson upper bound for all other gas pairs investigated (**Figure 1** and **S12**).

In contrast, OMe-ROMP exhibited significantly lower gas permeabilities compared to CF₃-ROMP and PIM-1 but higher permselectivities (**Figure 1** and **S11d**). These striking differences in transport properties are notable because CF₃-ROMP and OMe-ROMP are structurally very similar with the main exception being the -CF₃ versus -OMe functionality. Quantitatively, gas permeabilities are 7-10 fold higher, depending on the gas, for the CF₃-ROMP. This difference in performance can be rationalized by the higher BET surface area of CF₃-ROMP arising from the random configuration of CF₃- and OMe-substituted side chains. The pendant -CF₃ group is bulkier and stiffer than -OMe,

which hinders interchain packing and reduces intrachain rotational freedom, thus leading to higher porosity. Fluorine-containing moieties are also known to have high solubilities for light gases, which could subsequently increase permeabilities in the framework of the solution-diffusion model.^[19–21] It may be the combination of these two effects that leads to the significant increase in gas permeabilities, similar to trends reported for certain polyimides and polycarbonates.^[22] Molecular mechanics simulations suggest side chain bending into “pocket-shapes” are a potentially pseudo-stable conformation (Section 4, ESI). We also hypothesize that the pendant $-\text{CF}_3$ groups may form localized fluorine-rich domains between side chain segments as a result of the curvature of the side chain in 3D (Scheme 1c). However, the stereochemistry of Diels-Alder reaction during side chain formation is disordered and hence there is a distribution of the shape and size of the pockets.

a)



b)

c)

This article is protected by copyright. All rights reserved.

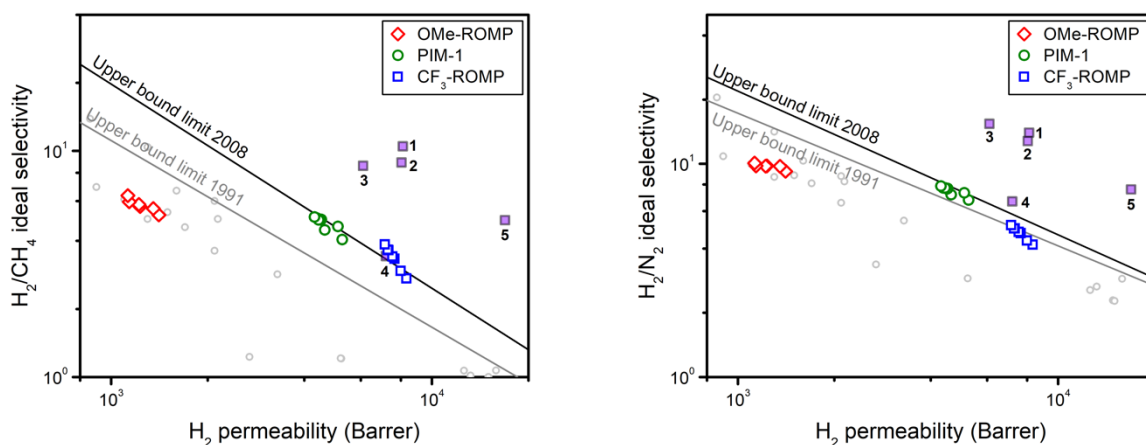


Figure 1. Robeson plots of CF₃-ROMP, OMe-ROMP, and PIM-1 for a) CO₂/CH₄ b) H₂/CH₄ c) H₂/N₂ gas pairs as a function of physical aging time. Black and gray lines represent 2008 and 1991 upper bounds, respectively.^[23,24] Filled purple squares represent other highly permeable PIMs reported: 1) PIM-EA-TB, 2) PIM-Trip-TB, 3) PIM-TMN-SBI, 4) PIM-TMN-Trip-TB 5) PIM-TMN-Trip.^[9,25]

Compared to PIM-1, CF₃-ROMP exhibited moderately lower selectivities for the gas pairs CO₂/CH₄, H₂/CH₄, and H₂/N₂. Diffusivity-selectivity and solubility-selectivity is presented in **Figure S19** and **S21**. According to **Figure 2, S13 and S14**, the solubility-selectivity of CF₃-ROMP is close to that of PIM-1 whereas its diffusivity-selectivity is lower for the majority of gas pairs. Considering the difference in pore-size distribution between two polymers (**Figure S6**), we hypothesize that the lower diffusivity-selectivity of CF₃-ROMP is most likely caused by polydispersity in length and stereochemistry of the side chains. Given this hypothesis, diffusivity-selectivity may be improved by homogenizing the length of side chains and devising systems that do not have structural variances as a result of the stereochemistry of the Diels-Alder reaction used in the side chain synthesis.

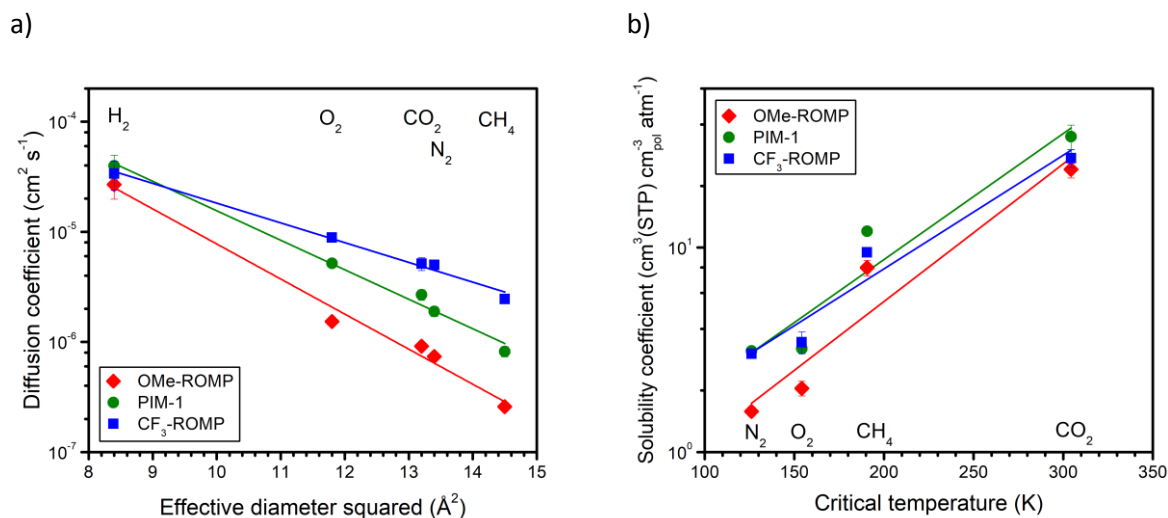


Figure 2. a) Diffusion coefficient plotted against effective diameter squared for CF₃-ROMP, OMe-ROMP, and PIM-1 at 1 h aging after liquid ethanol soaking for 48 h, air-drying for 24 h, and subjected to full vacuum for 8 h at 35 °C. The steepness of the slope indicates molecular sieving capabilities, thus molecular sieving capabilities decrease in the following order: -OMe > PIM-1 > -CF₃. b) Solubility coefficient of N₂, O₂, CH₄, and CO₂ in polymers as a function of critical temperature.

In addition to evaluating performance relative to the upper bounds, determining the effects of penetrant-induced plasticization is an important concern in membrane-based gas separations.^[26] Exposure of membranes to strongly interacting gases such as CO₂ at high pressures can reduce permselectivity as a result of sorption-induced swelling.^[27] Thus, membranes that maintain stable performance under high CO₂ feed pressures are desirable. In **Figure 3a**, CF₃-ROMP, OMe-ROMP and PIM-1 were subjected to CO₂ feed pressure up to 51 bar. Of note, CO₂ permeabilities of CF₃-ROMP decreased monotonically up to 51 bar even when using fugacity to account for non-idealities (**Figure S25**). This result reveals that the plasticization pressure point, above which permeability starts to

increase, was not reached under the conditions considered for these experiments. PIMs and many other non-crosslinked porous polymers exhibit plasticization pressure points at significantly lower pressures (**Figure S23** and **Table S2**), but the non-crosslinked CF₃-ROMP and OMe-ROMP have plasticization pressure points more characteristic to those of chemically-crosslinked polyimides.^[28,29] Moreover, when the CO₂ feed pressure was gradually decreased, the hysteresis induced by conditioning up to 51 bar was ~35% of the original CO₂ permeability. OMe-ROMP shows similar anti-plasticization behavior with plasticization pressure points > 51 bar, but the hysteresis (~50%) is slightly higher than CF₃-ROMP. As a comparison, the plasticization pressure point for PIM-1 when tested under identical conditions was ~27 bar, and it shows a significantly larger hysteresis effect (up to 95% increased permeability) when CO₂ feed pressure is released. These results indicate that the interchain cohesive energy for ROMPs is larger than that of PIM-1. This feature may originate from both a fluorophilic interaction between -CF₃ moieties and a greater rigidity-promoting “physical interlocking” between side chains typical of both ROMPs. Such an interpretation is in agreement with the results of Swaidan *et al.*, wherein interchain rigidity contributed to CO₂ plasticization resistance.^[12,30] To further investigate the plasticization resistance of CF₃-ROMP, 50:50 vol.% CO₂/CH₄ mixed-gas permeation experiments were run, and the details can be found in Section 11 of the ESI.

It is well-known that the relaxation of non-equilibrium free volume elements in PIMs proceeds rapidly in the first ~10 days after swelling in a non-solvent (*e.g.*, alcohols).^[31] To evaluate such behavior in the samples considered here, physical aging of CF₃-ROMP, OMe-ROMP, and PIM-1 was monitored by gas permeation measurements and wide-angle X-ray scattering (WAXS) for 2000 h. **Figure 3b** displays helium permeability as a function of the time, and it is clear that CF₃-ROMP, OMe-ROMP, and PIM-1 age at different rates. For smaller gases like He, H₂, and O₂, CF₃-ROMP aged

the slowest among samples considered, while OMe-ROMP aged the fastest with PIM-1 displaying intermediate behavior (**Figure S17**). Notably, the aging rate of CF₃-ROMP is significantly lower than that of state-of-the-art PIMs, although the alcohol treatment was slight different (ethanol vs. methanol).^[9,32] For instance, helium permeability decreased by ~45 % after 1000 h aging for PIM-TMN-Trip, whereas CF₃-ROMP only decreased by ~10 %. Moreover, the CF₃-ROMP films considered here are thinner than PIM-TMN-Trip (119 μm vs. 192 μm), and physical aging is accelerated for thinner films.^[33] For larger molecules like CO₂, N₂, and CH₄, there was no significant difference in aging rates between the three polymers compared in this work (**Figure S17a**). These findings suggest that using permeability as a proxy for assessing aging rates instead of diffusion is a limitation for more strongly sorbing components that also have significant solubility contributions to permeability.

Previous studies have shown that the introduction of fluorinated moieties can suppress physical aging in aromatic polyimides.^[34,35] In the case at hand, despite its higher BET surface area, the aging rate of CF₃-ROMP was considerably lower than that of OMe-ROMP for gases with smaller effective diameters. The WAXS of CF₃-ROMP displays a decrease in scattering intensity only over the larger *d*-spacing regime during physical aging, whereas OMe-ROMP exhibited a decrease in scattering intensity across the entire *d*-spacing range (**Figure S22**). This trend suggests that subtle differences in polymer chemistry for a similar polymer design may result in multiple, complex aging pathways. The reduced aging rate for CF₃-ROMP compared to OMe-ROMP likely results from a stability of CF₃-ROMP to contraction of smaller free volume elements (**Figure S15 and S16**).

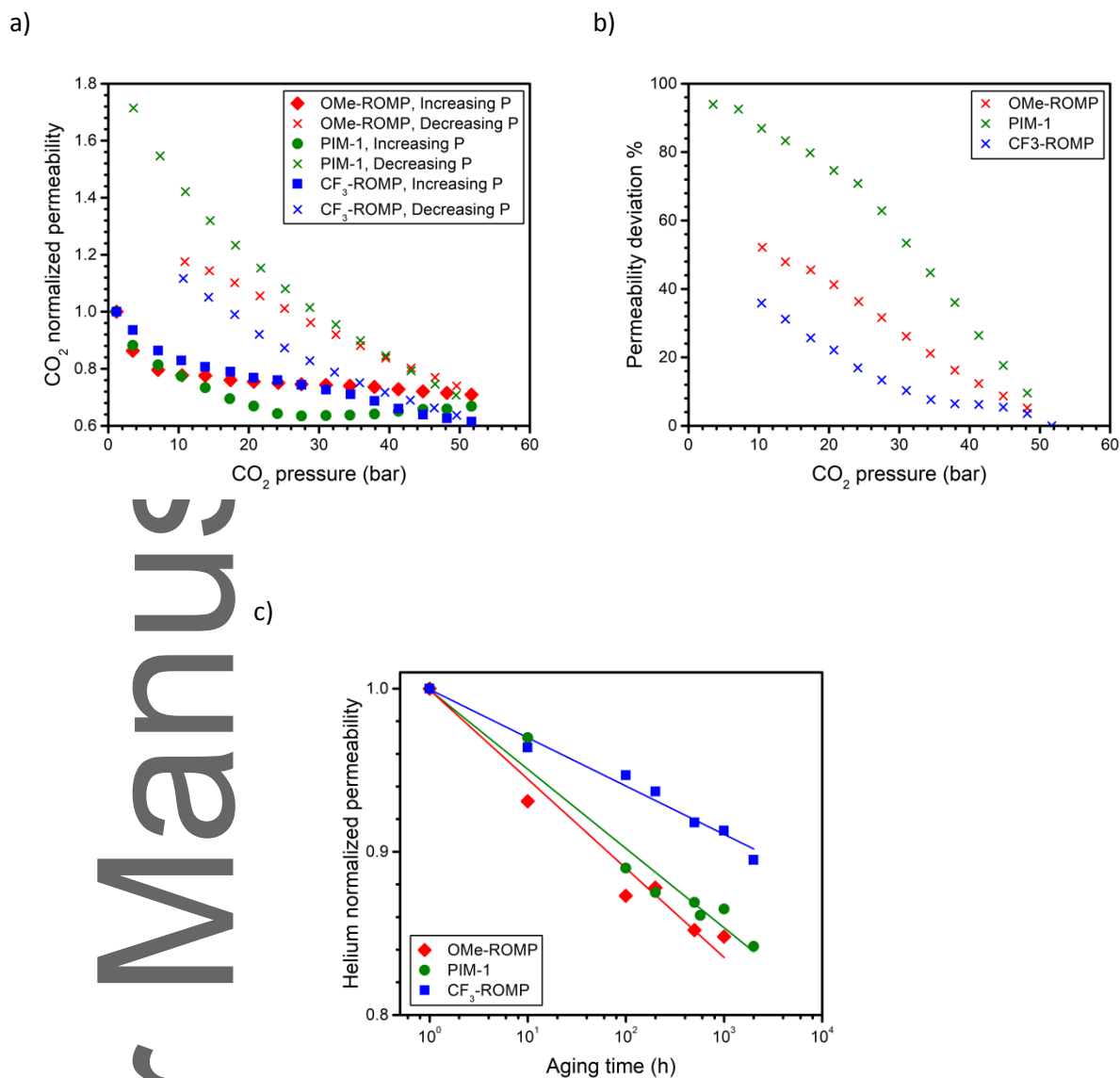


Figure 3. a) CO_2 plasticization study and b) hysteresis induced by conditioning of the film at 51 bar of CO_2 for CF_3 -ROMP, OMe-ROMP, and PIM-1. c) Physical aging study of helium by monitoring permeability over time for CF_3 -ROMP, OMe-ROMP, and PIM-1 between 1 and 2000 h after liquid ethanol treatment.

In summary, this communication demonstrates a versatile approach to achieve ultrahigh CO₂ permeabilities and selective size-sieving behavior for gas-phase separations by using pore-forming side chains attached to flexible polymer backbones. Pendant -CF₃ groups enhance gas permeability and reduce physical aging compared to their -OMe counterparts. The different performance metrics as a function of pendant groups on the side chain reveal that these features can be used to tailor gas separation performance. Outstanding plasticization resistance is a common feature for both of the ROMP polymers presented, indicating that this new structural design may provide a material platform to systematically address challenges with plasticization. Moreover, CF₃-ROMP exhibited a reduction in physical aging rate compared to PIM-1 even though it is characterized by significantly higher intrinsic permeabilities. The formation of porous polymers based on flexible backbones and rigid free volume promoting side chains represents a promising new platform of materials for addressing fundamental limitations in current design strategies for membrane materials.

Experimental Section

Synthesis of Porous ROMP polymers: Synthetic procedures for CF₃-ROMP and OMe-ROMP have been previously reported by Zhao and He *et al.*^[11]

Modelling and Gas Transport Properties: The 3D structure of CF₃-ROMP is optimized using the MMFF 94 force field as implemented in Avogadro 1.2.0.

Gas Transport Properties: Self-standing films of CF₃-ROMP, OMe-ROMP, and PIM-1 were prepared by slow evaporation of a 3 wt % polymer solution in chloroform using a flat aluminum Petri dish. The as-cast film was soaked in liquid ethanol before testing gas permeability and WAXS. TGA

analysis was performed to ensure the complete removal of residual solvents from the films and to determine their thermal stability. The thicknesses of CF₃-ROMP, OMe-ROMP, and PIM-1 films, as measured with a digital micrometer, were 119 μm, 160 μm, and 119 μm, respectively. Permeability was measured at 35 °C with a fixed-volume variable-pressure Maxwell Robotics automated permeation system from the slope of the curve (p, t) in the steady-state region after 6 times the time lag (θ). Pressure was measured with a MKS transducer (Model 622C, 10 Torr limit). The diffusion coefficient, \mathcal{D} , was determined by applying the time-lag method: $\mathcal{D} = l^2/6\theta$ where l is the film thickness. The solubility coefficient, \mathcal{S} , was determined in the framework of the solution-diffusion model where $\mathcal{S} = \mathcal{P}/\mathcal{D}$. Aging experiments were systematically performed on samples subjected to the same treatment and storage conditions, experiencing the same history for up to 2000 h. CO₂-induced plasticization experiments were performed by pressurizing samples up to 51 bar and depressurizing down to 1 bar to evaluate the hysteresis.

Supporting Information

Supporting Information is available from the Wiley Online Library or from the author.

Acknowledgements

Y.H. and F.M.B. contributed equally to this work. The authors declared the following competing financial interest(s): a patent has been filed on the polymers reported in this paper and their gas separation applications. F.M.B acknowledges the Marco Polo Scholarship by Department of Civil, Chemical, Environmental and Materials Engineering, Alma Mater Studiorum, University of Bologna.

We are grateful to Ashleigh L. Ward, Stephen M. Meckler, Mark Carrington, and Brett A. Helms for providing PIM-1 sample used in this work. Work at the Molecular Foundry, including PIM-1 synthesis

This article is protected by copyright. All rights reserved.

and characterization, was supported by the Office of Science, Office of Basic Energy Sciences, of the U.S. Department of Energy under Contract No. DE-AC02-05CH11231.

We are grateful to Prof. Haiqing Lin and Liang Huang at the University of Buffalo for assisting with mixed-gas experiments.

This work is supported by National Science Foundation through award DMR-1410718

Transport characterization work by S.L. is supported in part by the U.S. Department of Energy, Office of Science, Office of Basic Energy Sciences, Separation Science program under Award Number DE-SC0019087

Received: ((will be filled in by the editorial staff))

Revised: ((will be filled in by the editorial staff))

Published online: ((will be filled in by the editorial staff))

References

- [1] M. Galizia, W. S. Chi, Z. P. Smith, T. C. Merkel, R. W. Baker, B. D. Freeman, *Macromolecules* **2017**, *50*, 7809.
- [2] Y. Yampolskii, *Macromolecules* **2012**, *45*, 3298.
- [3] C. G. Bezzu, M. Carta, A. Tonkins, J. C. Jansen, P. Bernardo, F. Bazzarelli, N. B. Mckeown, *Adv. Mater.* **2012**, *24*, 5930.
- [4] S. Wang, X. Li, H. Wu, Z. Tian, Q. Xin, G. He, D. Peng, S. Chen, Y. Yin, Z. Jiang, M. D. Guiver, *Energy Environ. Sci.* **2016**, *9*, 1863.
- [5] N. B. McKeown, P. M. Budd, *Chem. Soc. Rev.* **2006**, *35*, 675.
- [6] Z. X. Low, P. M. Budd, N. B. McKeown, D. A. Patterson, *Chem. Rev.* **2018**, *118*, 5871.
- [7] T. M. Long, T. M. Swager, *J. Am. Chem. Soc.* **2003**, *125*, 14113.

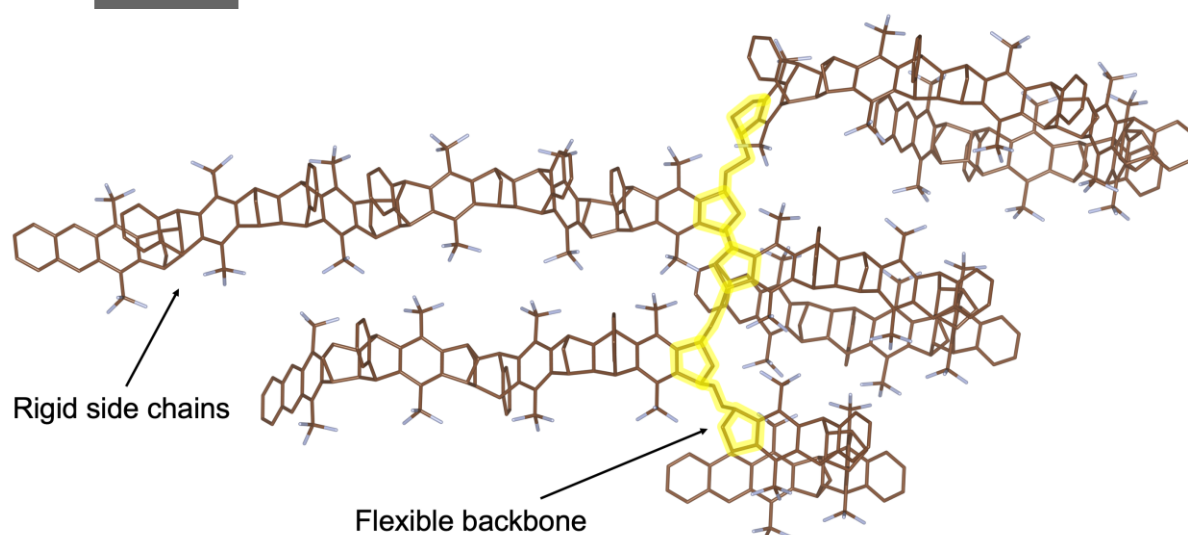
This article is protected by copyright. All rights reserved.

- [8] P. M. Budd, B. S. Ghanem, S. Makhseed, N. B. McKeown, K. J. Msayib, C. E. Tattershall, *Chem. Commun.* **2004**, 4, 230.
- [9] I. Rose, C. G. Bezzu, M. Carta, B. Comesanã-Gándara, E. Lasseuguette, M. C. Ferrari, P. Bernardo, G. Clarizia, A. Fuoco, J. C. Jansen, K. E. Hart, T. P. Liyana-Arachchi, C. M. Colina, N. B. McKeown, *Nat. Mater.* **2017**, 16, 932.
- [10] S. Liu, Z. Jin, Y. C. Teo, Y. Xia, *J. Am. Chem. Soc.* **2014**, 136, 17434.
- [11] Y. Zhao, Y. He, T. M. Swager, *ACS Macro Lett.* **2018**, 300.
- [12] R. Swaidan, B. Ghanem, M. Al-Saeedi, E. Litwiller, I. Pinnau, *Macromolecules* **2014**, 47, 7453.
- [13] N. Du, H. B. Park, G. P. Robertson, M. M. Dal-Cin, T. Visser, L. Scoles, M. D. Guiver, *Nat. Mater.* **2011**, 10, 372.
- [14] B. D. Freeman, *Macromolecules* **1999**, 32, 375.
- [15] M. G. Dhara, S. Banerjee, *Prog. Polym. Sci.* **2010**, 35, 1022.
- [16] J. R. Wiegand, Z. P. Smith, Q. Liu, C. T. Patterson, B. D. Freeman, R. Guo, *J. Mater. Chem. A* **2014**, 2, 13309.
- [17] S. Alexander Stern, *J. Memb. Sci.* **1994**, 94, 1.
- [18] C. R. Mason, L. Maynard-Atem, N. M. Al-Harbi, P. M. Budd, P. Bernardo, F. Bazzarelli, G. Clarizia, J. C. Jansen, *Macromolecules* **2011**, 44, 6471.
- [19] M. F. Costa Gomes, A. A. H. Pádua, *J. Phys. Chem. B* **2003**, 107, 14020.
- [20] D. F. Sanders, Z. P. Smith, R. Guo, L. M. Robeson, J. E. McGrath, D. R. Paul, B. D. Freeman, *Polymer* **2013**, 54, 4729.
- [21] J. G. Wijmans, R. W. Baker, *J. Memb. Sci.* **1995**, 107, 1.
- [22] M. W. Hellums, W. J. Koros, G. R. Husk, D. R. Paul, *J. Memb. Sci.* **1989**, 46, 93.
- [23] L. M. Robeson, *J. Memb. Sci.* **1991**, 62, 165.
- [24] L. M. Robeson, *J. Memb. Sci.* **2008**, 320, 390.
- [25] M. Carta, M. Croad, R. Malpass-Evans, J. C. Jansen, P. Bernardo, G. Clarizia, K. Friess, M. Lanč, N. B. McKeown, *Adv. Mater.* **2014**, 26, 3526.
- [26] J. K. Adewole, A. L. Ahmad, S. Ismail, C. P. Leo, *Int. J. Greenh. Gas Control* **2013**, 17, 46.

- [27] N. Du, M. M. Dal-Cin, G. P. Robertson, M. D. Guiver, *Macromolecules* **2012**, *45*, 5134.
- [28] W. Qiu, C. C. Chen, L. Xu, L. Cui, D. R. Paul, W. J. Koros, *Macromolecules* **2011**, *44*, 6046.
- [29] A. M. Kratochvil, W. J. Koros, *Macromolecules* **2008**, *41*, 7920.
- [30] R. Swaidan, B. Ghanem, E. Litwiller, I. Pinnau, *Macromolecules* **2015**, *48*, 6553.
- [31] P. Bernardo, F. Bazzarelli, F. Tasselli, G. Clarizia, C. R. Mason, L. Maynard-Atem, P. M. Budd, M. Lanč, K. Pilnáček, O. Vopička, K. Friess, D. Fritsch, Y. P. Yampolskii, V. Shantarovich, J. C. Jansen, *Polymer* **2017**, *113*, 283.
- [32] N. B. M. Mariolino Carta, Richard Malpass-Evans, Matthew Croad, Yulia Rogan, Johannes C. Jansen, Paola Bernardo, Fabio Bazzarelli, *Science* **2013**, *339*, 1095.
- [33] Y. Huang, D. R. Paul, *Polymer* **2004**, *45*, 8377.
- [34] J. H. Kim, W. J. Koros, D. R. Paul, *Polymer* **2006**, *47*, 3094.
- [35] H. Lin, *Curr. Opin. Chem. Eng.* **2014**, *4*, 54.

TOC text

A porous polymer featuring a flexible backbone and rigid, fluorinated side-chains is prepared via Ring-Opening Metathesis Polymerization (ROMP). This polymer exhibits ultrahigh CO₂ permeability (> 21000 Barrer) and exceptional plasticization resistance (CO₂-induced plasticization pressure > 51 bar). By generating ultramicroporosity through pre-designed side chains instead of the polymer backbone, a promising new design strategy is presented for gas-separation membranes.



This article is protected by copyright. All rights reserved.